

## ORIGINAL ARTICLE

# Dose Selection Based on Modeling and Simulation for Rivipansel in Pediatric Patients Aged 6 to 11 Years With Sickle Cell Disease

Brinda K. Tammara<sup>1</sup> and Lutz O. Harnisch<sup>2\*</sup>

This modeling and simulation exercise aimed to provide dosing recommendations for rivipansel phase III studies in children aged 6–11 years with sickle cell disease (SCD). Pharmacokinetic data from 109 patients aged 12–51 years who received rivipansel (2–40 mg/kg) in previous studies (three phase I and one phase II) were integrated to build a three-compartmental simulation model. Renal clearance simulations across the age range accounted for renal function development and postulated hyperfiltration in SCD. Simulated demographic distributions for the pediatric SCD population were used to predict concentration-time profiles from three dosing regimens, which were then compared against efficacious average steady-state concentrations observed in phase II. A dosing regimen comprising a 40-mg/kg loading dose followed by a 20-mg/kg maintenance dose every 12 hours was selected, as it will likely provide an efficacious concentration range. Its validity will be confirmed in the ongoing phase III study.

CPT Pharmacometrics Syst. Pharmacol. (2017) 6, 845–854; doi:10.1002/psp4.12263; published online 8 November 2017.

## Study Highlights

### WHAT IS THE CURRENT KNOWLEDGE ON THE TOPIC?

☑ A population PK model for rivipansel in SCD was described in adults and the impact of SCD on growth and GFR in terms of hyperfiltration has been described in the literature.

### WHAT QUESTION DID THIS STUDY ADDRESS?

☑ How to derive a dose selection rationale for a rivipansel phase III study that includes pediatric patients with SCD aged 6–11 years, in the absence of PK information in that population.

### WHAT THIS STUDY ADDS TO OUR KNOWLEDGE

☑ A population PK model from a previous phase II study combined with knowledge of the pathophysiology of the

disease and its utilization in a modeling and simulation exercise for dose selection.

### HOW MIGHT THIS CHANGE DRUG DISCOVERY, DEVELOPMENT, AND/OR THERAPEUTICS?

☑ Exemplify a path to integrate knowledge of study data and use of disease-specific (SCD) and population-specific (pediatrics/African American) information in a quantitative way to inform dose selection in the target population, which may eliminate the need for a separate dose-finding study in diseased children, hence improving patient utilization and reducing development time and cost. The presented concept and application could very well be applicable to other therapeutic areas.

Sickle cell disease (SCD) is the most common inherited RBC (RBC) disorder and affects individuals of African, Mediterranean, and Asian descent.<sup>1</sup> Clinical manifestations of SCD include recurrent painful crises, chronic hemolytic anemia, acute chest syndrome, pulmonary hypertension, stroke, kidney failure, priapism, leg ulcers, osteonecrosis, and cardiac disease.<sup>2–4</sup>

Selectin-dependent intercellular adhesion contributes to vaso-occlusion, which is a major cause of organ damage in SCD.<sup>5</sup> Interactions between sickled RBCs, leucocytes, and endothelial cells are mediated by multiple adhesion molecules.<sup>6</sup> The vascular endothelium is activated in SCD, and its role in the pathology of this disease has been reported.<sup>7</sup> There is upregulation of adhesion molecules, such as VCAM, P-selectin, and E-selectin, which bind adhesion molecules on RBCs and on polymorphonuclear lymphocytes.<sup>7</sup> Inhibition of E-selectin, P-selectin, and L-selectin, a pan-selectin inhibition approach, offers potential as a therapeutic

option in sickle cell vaso-occlusive crisis (VOC). Data in the literature support a key role for selectins in VOCs. In particular, Turhan *et al.*<sup>8</sup> suggested that drugs affecting leukocyte-endothelial interactions or leukocyte-sickle RBC aggregation may have an important role in the treatment of VOCs.<sup>8</sup> Because this a genetic disease, children and adults have very similar disease characteristics, but complications increase with age, leading to early mortality. Infants with SCD can present with symptoms beginning at 6 months of age (as fetal hemoglobin dissipates) with dactylitis (painful swelling of the hands or feet), anemia, mild jaundice, or an enlarged spleen.<sup>9</sup>

Hyperfiltration is an abnormal increase in the filtration rate of the renal glomeruli and baseline glomerular filtration rate (GFR) measurements suggest that renal dysfunction in SCD, evidenced by glomerular hyperfiltration, begins during infancy.<sup>10</sup> The majority of the children with SCD have

<sup>1</sup>Pfizer, Collegeville, Pennsylvania, USA; <sup>2</sup>Pfizer, Sandwich, UK. \*Correspondence: L O Harnisch ([Lutz.O.Harnisch@pfizer.com](mailto:Lutz.O.Harnisch@pfizer.com))  
Received 6 July 2017; accepted 23 October 2017; published online on 8 November 2017. doi:10.1002/psp4.12263

documented hyperfiltration starting early in life, but the degree of hyperfiltration may depend on several factors, including the genotype of SCD.<sup>11,12</sup>

There are a few investigational drugs in development, but currently, hydroxyurea is the only approved drug for treatment of SCD.<sup>13</sup>

Rivipansel is a pan-selectin antagonist found to inhibit selectin binding *in vitro* and inhibit selectin-mediated effects *in vivo*. Rivipansel is under development for treatment of VOC in patients with SCD.

Rivipansel has a low volume of distribution in all species (mouse, rat, monkey, minipig, and human), with a protein binding of about 60%. No *in vitro* metabolism in hepatocytes (rat, monkey, and human) was observed. Renal excretion of unchanged drug (>90% of dose in urine) is the primary clearance mechanism. The mean half-life from phase I studies is 7–8 hours, with no dose-related trends seen in either clearance or half-life (studies 101 and 102, unpublished data). The volume of distribution at steady state ( $V_{ss}$ ) following a single 4 g i.v. dose of rivipansel was 12 L and the clearance was 1.3 L/hr.<sup>14</sup>

In a multicenter, randomized, double-blind, placebo-controlled phase II study of rivipansel (NCT01119833),<sup>15</sup> consistent, clinically meaningful reductions in multiple measures of VOC were observed in patients receiving rivipansel compared with those receiving standard of care treatment.

Although the phase II study included 12 children aged 12–17 years only, the pivotal, randomized, double-blind phase III study planned to also enroll children aged 6–11 years. The present modeling and simulation exercise was conducted to develop rivipansel dosing recommendations for these younger children in the phase III study. The authors would like to emphasize that the main focus of this manuscript is the simulation exercise performed for phase III dose selection in pediatric patients aged 6–11 years, and not a population pharmacokinetic (PK) model building exercise.

## METHODS

### Study design and data sources

For this study, PK data from four prior rivipansel studies (three phase I and one phase II) were used. Two phase I studies (unpublished data; Pfizer, Collegeville, PA) evaluated rivipansel in healthy adult volunteers after either a single i.v. dose (study 101;  $n = 40$ ; doses ranged from 2–40 mg/kg) or after multiple i.v. doses (study 102;  $n = 32$ ; doses ranged from 2–20 mg/kg every 8 hours and a 40-mg/kg loading dose followed by 20 mg/kg every 8 hours) compared to placebo. A third phase I study (study 103; NCT00911495) evaluated rivipansel in adults with SCD after two i.v. doses ( $n = 15$ ; 20-mg/kg loading dose followed by a 10-mg/kg dose after 10 hours) who were not experiencing a VOC.<sup>16</sup>

In the phase II study (NCT01119833),<sup>15</sup> two dose levels of i.v. rivipansel (the first cohort received a 20-mg/kg loading dose, followed by 10 mg/kg every 12 hours for 7 days and the second cohort received a 40-mg/kg loading dose followed by 20 mg/kg every 12 hours for 7 days) or placebo were administered to patients with SCD aged 12–60 years who were hospitalized for VOCs ( $n = 76$ ; 56 adults and 20 children).

Data were integrated to build a three-compartmental model, which was used to perform simulations across a range of potential doses. This integrated population PK model was developed using a nonlinear, mixed-effects modeling approach, as implemented in the NONMEM software system version 7.3.0 (ICON Development Solutions, Hanover, MD), using first-order conditional estimation with interaction and an additive + proportional residual variability model. In addition, R software version 3.2.2 (The R Foundation, Vienna, Austria) was used as the interface for data manipulation and graphing.

Two independent analyses on the phase I and phase II data (unpublished data; Pfizer) were available prior to our own assessments. We combined the two datasets to create an integrated single population PK model that allowed the extrapolation to the pediatric population, aged 6–11 years, included in the ongoing phase III study. We had kept the structural components (the three-compartmental model from previous analyses) and variance components, but re-estimated all parameters to arrive at a model fit-for-purpose, as confirmed by model diagnostics. More details about the structure and model building sequence of the integrated PK model are provided as part of **Supplementary Figures S1–S11 and Tables S1 and S2**. The precision of parameter estimates was initially obtained from the covariance step in NONMEM, but for the final model, SEs and confidence intervals (CIs) were estimated using the sampling importance resampling (SIR) procedure.<sup>17</sup>

Because rivipansel is primarily eliminated renally, the model took into account the distribution of demographic variables (gender, height, weight, and creatinine levels) essential for defining clearance across the proposed age range. In this model, clearance was described as a function of creatinine clearance (CRCL) and distributional volumes were described as a function of weight. Additionally, hyperfiltration has been reported in patients with SCD, including children,<sup>18,19</sup> which likely has an impact on the GFR and elimination of rivipansel. In the previous rivipansel studies, a difference in clearance between healthy volunteers and patients with SCD was observed, which may in part be a reflection of the hyperfiltration. Assuming the presence of hyperfiltration at a similar magnitude, this factor (about 23%) was also applied to children in the PK model and simulation exercise.

In the present model, CRCL (mL/min) in adults was estimated using the Cockcroft-Gault formula<sup>20</sup>:

$$\text{CRCL (mL/min)} = (140 - \text{AGE}) \cdot \text{WT} / (72 \cdot \text{SeCr}) \cdot (0.85 \text{ (if female)})$$

wherein AGE is age in years, WT is weight (kg), and SeCr is serum creatinine level (mg/dL).

To estimate CRCL (mL/min) in children, the Schwartz formula<sup>21</sup> adjusted for individual body surface area (BSA) was used as:

$$\text{CRCL (mL/min)} = 0.413 \cdot \text{HT} / \text{SeCr} \cdot \text{BSA} / 1.73 \text{ m}^2$$

wherein HT is height (cm), SeCr is serum creatinine level in mg/dL, and BSA is the individual body surface area calculated according to Dubois and Dubois.<sup>22</sup> By applying the BSA adjustment to the Schwartz formula, the two calculations predicted absolute CRCL necessary to align the

values across the full age range. CRCL was the better predictor of total clearance than any relationship with weight only.

To generate distributions of the demographics to be used in the simulations based on the model, the following approaches were taken: the covariance matrix of demographics (age, weight, height, and creatinine levels across both genders), as observed in the phase II study, was used to simulate demographics in older children (aged 12–17 years) and in adults in the SCD target population. To derive a demographic distribution in children at a given age, median and variance values across gender and age groups were obtained from growth charts developed by the US Centers for Disease Control and Prevention (CDC).<sup>23</sup> In addition, to assess the validity of the chosen demographic distribution for a largely black population, the CDC growth charts were compared against information in the literature characterizing children with SCD, including data from the Cooperative Study on SCD<sup>24</sup> and a subpopulation of Jamaican children with SCD.<sup>25</sup>

To derive a relevant CRCL distribution, creatinine changes with age were also considered as follows: data on creatinine changes with age in children are limited, especially in children with SCD. A summary paper on reference values for creatinine concentrations by Ceriotti *et al.*<sup>26</sup> references one small German cohort in largely healthy children,<sup>27</sup> whereas Hoste *et al.*<sup>28</sup> describe more recently a larger Belgian cohort of nearly 16,000 children and young adults. Normal ranges, according to Mayo Medical Laboratories<sup>29</sup> or Hoste *et al.*<sup>28</sup> begin to differ between boys and girls around the age of 10 years, but reach values of about 0.75 µg/mL and 0.65 µg/mL, respectively, at about 15 years, which is higher than values seen in children with SCD. We used the relationship from Hoste *et al.*<sup>28</sup> and applied a triangular linear reduction starting at 6 years and reaching at 16 years 0.1 mg/dL in boys and 0.15 mg/dL in girls, respectively. This modified relationship reflected lower creatinine values as observed in our own phase II study in children and adults, but also the range of values observed in the Cooperative Study on SCD.<sup>24</sup> The original and resulting relationship between creatinine and age are presented in **Supplementary Figure S1**.

The derivation of the individual typical clearance values according to the population PK model follows as:

$$TV.CL (L/h) = 1.25 \cdot (CRCL/150)^{0.468} \cdot (1.234 \text{ (if SCD patient)})$$

with the typical value multiplied by  $\eta$ , as sampled from a log-normal distribution, with mean zero and SD of 19%, as estimated in the population PK model.

### Simulation exercise and derivation of target exposure ranges

Rivipansel is administered as a 20-minute i.v. infusion. The range of dosing regimens explored for children aged 6–11 years included: (1) a 20-mg/kg loading dose of rivipansel followed by a 10-mg/kg maintenance dose given every 12 hours (20/10 mg/kg); (2) a 30-mg/kg loading dose of rivipansel followed by a 15-mg/kg maintenance dose every 12 hours (30/15 mg/kg); and (3) a 40-mg/kg loading dose of rivipansel followed by a 20-mg/kg maintenance dose every 12 hours (40/20 mg/kg). The low dose corresponded

to the lower dose given in the phase II study, and the highest dose was limited by preclinical toxicity, with the third dose placed at the midpoint between the two.

In the ongoing phase III program, adults and children aged 12 years and older receive a fixed 1680-mg loading dose followed by an 840-mg maintenance dose administered every 12 hours. As a child younger than 12 years weighing more than 42 kg would receive a weight-based maintenance dose >840 mg, the maximum dosage for any child was capped at the adult dosage (1680-mg loading dose, 840-mg maintenance dose given every 12 hours).

Consistent with the phase III dosing regimen, all simulated dosing regimens were based on a single loading dose, with 5 subsequent maintenance doses administered every 12 hours as steady-state concentrations were reached by day 3. Concentrations were determined from the simulation after the last dose at the end of the 20-minute infusion (maximum drug concentration in the dosing interval ( $C_{max}$ )), and at 11.5 hours after the end of the infusion (minimum drug concentration in the dosing interval ( $C_{min}$ )), with the average concentration within a dosing interval at steady-state ( $C_{avg,ss}$ ) calculated from simulated individual clearances as:

$$C_{avg,ss} [\mu g/mL] = Dose_i / Cl_i \cdot 2/24$$

wherein  $Dose_i$  and  $Cl_i$  represent individual dose and clearance.

Simulations were summarized by age for children aged 6–11 years. Simulations for children aged 12–17 years were summarized in one group and adults in another. We simulated 10,000 subjects for the age range 6–17 years, and 10,000 subjects from the demographic covariance matrix from phase II, the latter retaining only subjects within the observed ranges in the trial. This resulted in each dosing regimen being simulated about 830 times for every age below 12 years, about 6,000 times for the 12–18 years old, and about 8,000 times for adults.

Although the  $C_{avg,ss}$  simulations did not contain residual error as they reflect a model-based summary measure across the whole dosing interval,  $C_{min}$  and  $C_{max}$  values were simulated including residual error to allow for a direct comparison with later summary reports from the currently ongoing phase III study.

### Assessing exposure distributions in pediatric patients

The exposure distributions from the three dosing regimens for children aged 6–11 years were compared against the following target criteria: achieving a concentration distribution ( $C_{avg,ss}$ ), as was observed with the lower dosage administered in the phase II study,<sup>15</sup> which seemed to be effective; achieving concentrations >10 µg/mL, based on preclinical efficacy data (improved blood flow and survival rate in SCD mice)<sup>30</sup>; and achieving similarity between exposure distributions for a given age when compared with the adult population treated with the 840-mg maintenance dose. The resulting  $C_{avg,ss}$  distributions were compared by visual inspection of the graphs across the criteria defined above. For reference, the corresponding distributions for  $C_{max}$  and  $C_{min}$  are provided as part of the **Supplementary Material**, and, in particular, the latter compared against the

**Table 1** Final parameter estimates for the integrated rivipansel population pharmacokinetic model

Parameter	Estimate	SIR %RSE <sup>a</sup>	SIR 95% CI <sup>a</sup>	
			Lower	Upper
<b>Structural model</b>				
CL, <sup>b</sup> L/h	1.25	2.12	1.2	1.3
V <sub>1</sub> , <sup>c</sup> L	6.24	2.83	5.91	6.6
Q <sub>rapid</sub> , L/h	2.62	5.86	2.34	2.96
V <sub>2</sub> , <sup>c</sup> L	4.02	2.72	3.8	4.24
Q <sub>slow</sub> , L/h	0.0316	17.5	0.0226	0.0441
V <sub>3</sub> , <sup>c</sup> L	0.656	7.85	0.563	0.76
<b>Covariate model</b>				
Study effect on CL, % difference if study 201	23.4	21.2	14.2	33.9
Exponent for CRCL on CL	0.468	15.9	0.325	0.619
Exponent for WT on V <sub>1</sub> , V <sub>2</sub> , and V <sub>3</sub> <sup>c</sup>	0.569	15.1	0.406	0.74
<b>Interindividual variability parameters<sup>d</sup></b>				
CL, %CV	18.8	15.4	16.3	21.8
V <sub>1</sub> , %CV	24.1	17.8	20.6	28.9
Q <sub>rapid</sub> , %CV	19.8	65.7	5.84	32.4
V <sub>2</sub> , %CV	15.5	26.8	11.9	19.7
Q <sub>slow</sub> , %CV	15.5	191	1.47	41.4
V <sub>3</sub> , %CV	15.3	63.5	5.61	24.4
<b>Residual variability parameters<sup>d</sup></b>				
Additive component of residual error, <sup>e</sup> for phase I studies, µg/mL	0.29	26.7	0.172	0.479
Additive component of residual error, <sup>e</sup> for study 201, µg/mL	0.165	70.7	0.0144	0.457
Proportional residual error, %CV for phase I studies	9.52	4.33	9.14	9.95
Proportional residual error, %CV for study 201	23.2	12	20.9	26.2

CI, confidence interval; CL, clearance; CRCL, creatinine clearance (ml/min); CV, coefficient of variation; Q<sub>rapid,slow</sub>, rapid or slow inter-compartmental clearances; RSE, relative standard error; SIR, sampling importance resampling; V<sub>1</sub>, volume of central compartment; V<sub>2,3</sub>, volumes of peripherals compartment; WT, weight (kg).

<sup>a</sup>RSE and CI for omega and sigma reported on the SD scale. <sup>b</sup>Typical CL for a subject is:  $CL = 1.25 \times (CRCL/150)^{0.468} \times (1 + 0.234 \times STUD)$ , where STUD = 1 for study 201 (otherwise = 0). <sup>c</sup>Typical V<sub>1,2,3</sub> for a subject are:  $V_1 = 6.24 \times (WT/70)^{0.569}$ ,  $V_2 = 4.02 \times (WT/70)^{0.569}$ , and  $V_3 = 0.656 \times (WT/70)^{0.569}$ .

<sup>d</sup>The  $\eta$ -shrinkage for interindividual variability ranged between 4.5% (CL) to 79% (Q<sub>rapid</sub>) and  $\epsilon$ -shrinkage was 7.8% for the model from phase I data and 11.9% for phase II data. <sup>e</sup>Concentration below which the additive component prevails on the residual error.

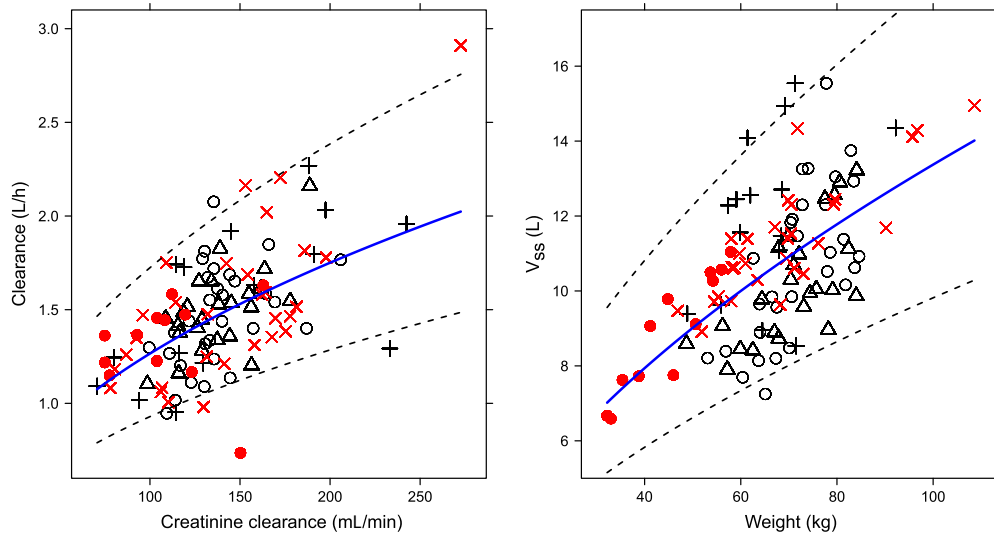


**Figure 1** Covariate relationship effects in the integrated population pharmacokinetic (PK) model. The two panels represent the estimated covariate relationships in the integrated population PK model. Left panel: clearance in patients with sickle cell disease (SCD) vs. creatinine clearance; right panel: volume at steady state ( $V_{ss}$ ) vs. weight. Lines correspond to mean and 95% prediction interval, symbols to individual clearance or  $V_{ss}$  Bayesian estimate values. Red symbols indicate patients from the phase II study (children aged 12–17 years: closed circles; adults, crosses), and black circles, triangles, and crosses indicate participants from each of the phase I studies. In the left panel, clearance values for the phase I studies have been prediction corrected on the estimated SCD factor between phase I and II of 23%.

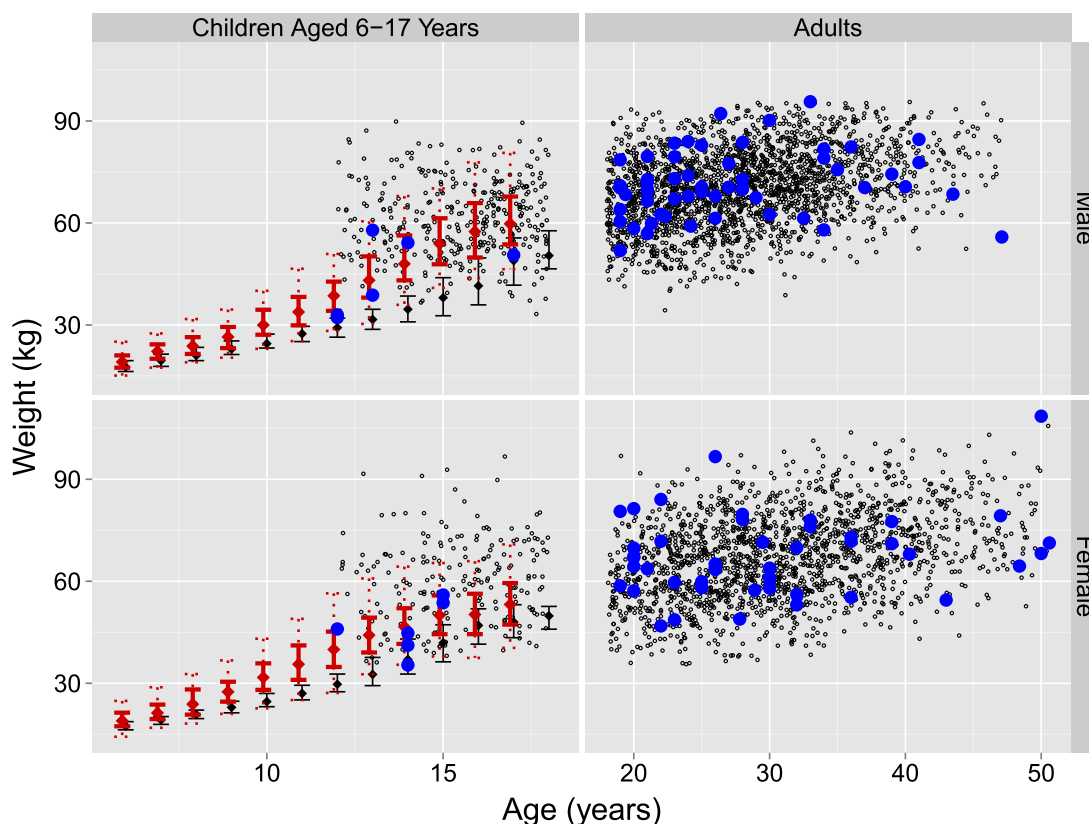


**Figure 2** Simulated weight distribution across the age ranges being studied in the ongoing phase III study. The left panels correspond to children aged 6–17 years, and the right panels correspond to adults. The top panels correspond to male subjects, and bottom panels to female subjects. Black dots represent simulations based on the covariance matrix constructed from the phase II patient population.<sup>15</sup> The blue dots across all panels represent patients from the phase II study. The black error bars represent median, 25th and 75th percentiles, as extracted from the literature on a Jamaican population<sup>25</sup> the red error bars summarize the simulations from Centers for Disease Control and Prevention tables similarly, but add dashed hinges at the 5th and 95th percentiles.<sup>23</sup>

prespecified target concentration of 10  $\mu\text{g/mL}$  ensuring a sufficient exposure during the whole dosing interval.

**Model assumptions.** Based on the Pediatric Study Decision Tree<sup>31</sup> developed by the US Food and Drug Administration, assumptions for studying young children in the ongoing phase III rivipansel study were made. For the present model, it was assumed that disease characteristics were similar in children and adults<sup>9</sup> and that children experience a response to treatment similar to that of adults (i.e., the mechanism of drug action is similar between children and adults with SCD). Additionally, similar efficacy was assumed to be achieved at similar drug exposure levels across all age ranges, with PK testing conducted and pharmacodynamic parameters measured in the adult and pediatric populations in the phase III study to confirm the validity of the assumptions.

To predict an appropriate dosing regimen in children, a similar structural population PK model was considered applicable in children and adults, and fixed effects in the population PK model estimated in adults were considered to apply to the scaling of exposure from adults to children. Additionally, the demographic distribution simulated from the phase II rivipansel study was assumed to be representative of the future phase III study population with SCD.

Variance assumptions estimated from the phase II study were considered applicable to the phase III study.

Following integration of the population PK model across all patients who received rivipansel in previous studies, we simulated exposure distributions across different dosing regimens across all ages and assessed the characteristics of the exposure distributions in pediatric patients.

## RESULTS

The current integrated population PK model is reliable for estimating the effects of covariates and extrapolating data into the pediatric domain. The final parameter estimates for the final integrated population PK model are provided in **Table 1**, with the renal clearance a function of CRCL and the volume of distribution a function of weight. The model resulted in very similar central parameters, fixed effects, and variability estimates compared with the earlier PK models. Details on goodness-of-fit, including visual predictive checks for the integrated PK model are provided in the **Supplementary Material**.

The distribution of individual parameters based on the final population PK model, particularly those relevant to the

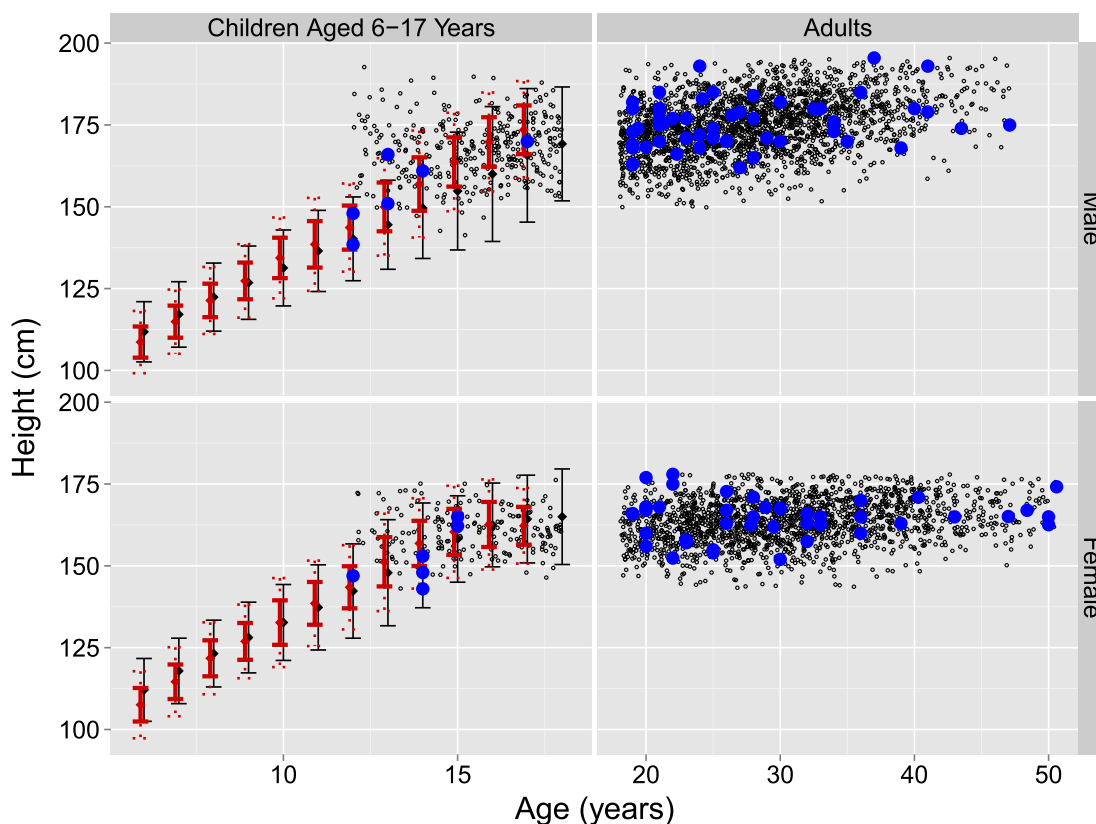


**Figure 3** Simulated height distribution across the age ranges being studied in the ongoing phase III study. The left panels correspond to children aged 6–17 years, and the right panels correspond to adults. The top panels correspond to male subjects, and the bottom panels correspond to female subjects. Black dots represent simulations based on the covariance matrix constructed from the phase II patient population.<sup>15</sup> The blue dots across all panels represent patients from the phase II study. The black error bars represent median and approximate 95% confidence intervals extracted from the literature on a Jamaican population.<sup>25</sup> The red error bars summarize the simulations from Centers for Disease Control and Prevention tables as mean and one (bars) and two (dashed hinges) SDs.

extrapolation of data into a young pediatric population, are presented in **Figure 1**. The relationship between clearance and volume of distribution and the corresponding covariates, as estimated from the integrated population PK model, is indicated in the graphs.

### Demographics

The distribution of weight and height for various ages, as extracted from the CDC tables, was used as a base from which to model the simulation of CRCL in a younger pediatric population, aged 6–11 years. The resulting distributions are presented in **Figure 2** and **Figure 3**. For comparison, a simulation of adult data based on the observed data from the phase II study is contrasted in the figures. In addition, an observed distribution in a Jamaican SCD population is added for comparison.<sup>25</sup> For the Jamaican population, a growth delay seemed to occur, which may be relevant for the target population and was reflected in a 5% lower weight and 1 year delay in the height changes as evidenced from the Cooperative Study on SCD.<sup>24</sup>

To reflect the pediatric creatinine distribution, we modified the relationship from Hoste *et al.*<sup>28</sup> in its dependency on age and gender to reflect the observed creatinine values from the phase II study in patients with SCD at the age of 12–18 years and adults, also accounting for the fact that

the Cooperative Study in patients with SCD<sup>24</sup> contains rather lower creatinine values in younger children, rarely exceeding 0.6 mg/dL. The resulting creatinine relationship with age is illustrated in **Supplementary Figure S1**. The full range of values, as used in the simulations after adding a variability of 18%, reflecting the variability, as observed in the phase II study, is depicted in **Supplementary Figure S2**.<sup>29,32</sup>

For the primary simulation exercise, clearance values were calculated in the same way as applied in the modeling exercise (Schwartz formula for children adjusted for BSA; Cockcroft-Gault formula for adults), ensuring that a size-related normalization is handled equivalently across the populations and between modeling and simulation exercises. The resulting distribution of CRCL levels across the age ranges is presented in **Figure 4**.

### Younger pediatric population PK simulation results

The simulated concentration-time profiles after different dosing regimens across the age ranges are shown in **Figure 5**. To allow a direct comparison across dosing regimens, box and whisker plots showing the  $C_{avg,ss}$  distribution achieved across the age range with the range of observed concentrations from phase II in the background are shown in **Figure 6**.

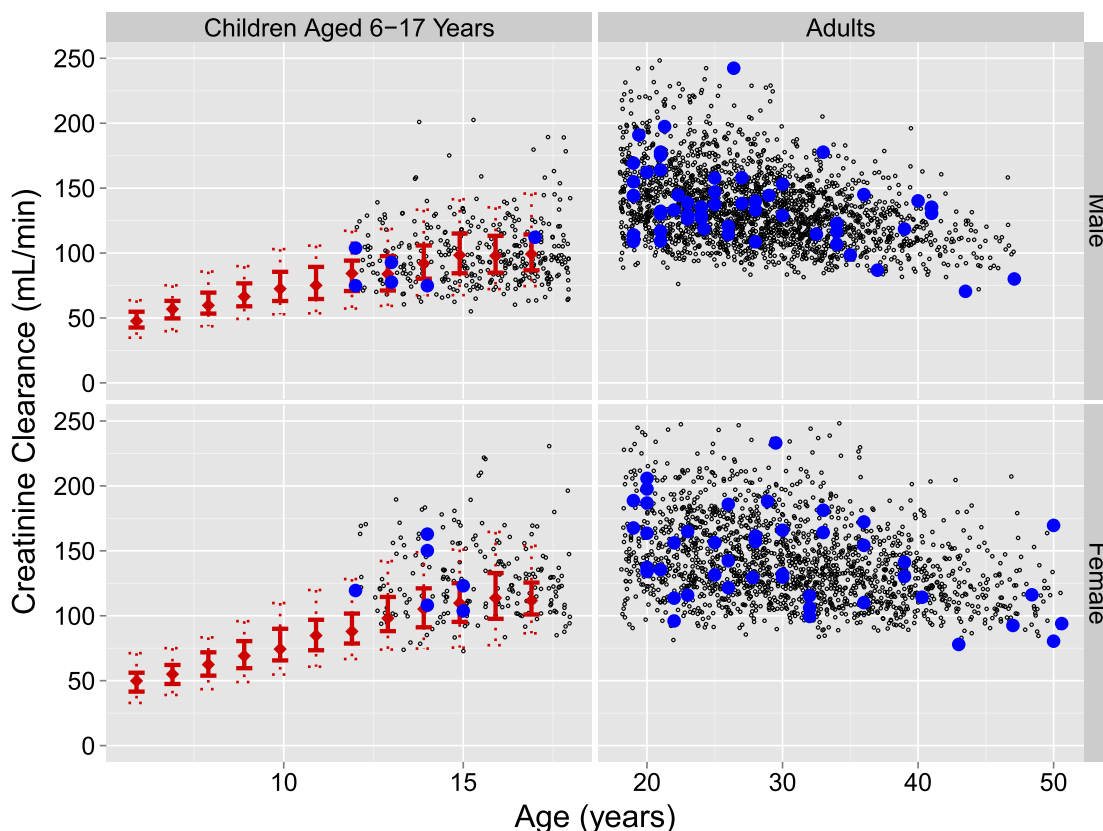


**Figure 4** Distribution of creatinine clearance levels, as calculated from simulation of weight, height, creatinine, and gender across the age ranges being studied in the ongoing phase III study. The left panels correspond to children aged 6–17 years, and the right panels to adults. The top panels correspond to male subjects, and the bottom panels to female subjects. Black dots represent the calculations based on simulations using the covariance matrix for weight, height, and creatinine constructed from the phase II patient population.<sup>15</sup> The blue dots across all panels represent values observed in the phase II study. Red error bars represent calculations based on simulations of weight, height from the Centers for Disease Control and Prevention tables<sup>23</sup> and creatinine based on the modified Hoste *et al.*<sup>28</sup> relationship indicating the median, 25th and 75th percentiles (bars), and 5th and 95th percentiles (dashed hinges).

For children aged 6–11 years, the 20-mg/kg loading dose followed by a 10-mg/kg every 12 hours maintenance dosing regimen is predicted to produce a  $C_{avg,ss}$  distribution that will fall below the target of 10  $\mu\text{g/mL}$  and will also result in a poor match to the  $C_{avg,ss}$  distribution observed in phase II.

The 30-mg/kg loading dose followed by a 15-mg/kg every 12 hours maintenance dosing regimen is predicted to produce a  $C_{avg,ss}$  distribution that will be above the target of 10  $\mu\text{g/mL}$  for children with SCD aged 9–11 years, and will also cover the  $C_{avg,ss}$  distribution observed in the phase II study for this age range. However, the children in the group aged 6–8 years will likely be at the lower end of the target range.

Finally, the 40-mg/kg loading dose followed by a 20-mg/kg every 12 hours maintenance dosing regimen is predicted to produce a  $C_{avg,ss}$  distribution that will be above the target of 10  $\mu\text{g/mL}$  for ages 6–11 years. For the age range of 9–11 years, the  $C_{avg,ss}$  distribution will be closer to matching the concentration distribution predicted for adults receiving the 840-mg maintenance dosing regimen.

For additional illustration, the distributions for  $C_{max}$  and  $C_{min}$  indicate that throughout the entire dosing interval

concentrations exceed the prespecified target concentration of 10  $\mu\text{g/mL}$  for the 40/20-mg/kg dose regimen in the 9–11 year old children, and only a fraction of the 6–8 year old children will experience concentrations below the target of 10  $\mu\text{g/mL}$  for part of their dosing interval.

## DISCUSSION

This modeling and simulation exercise was conducted to identify a dosing regimen of rivipansel suitable for use in pediatric patients with SCD who will participate in the ongoing phase III study. Under the assumption that disease progression for SCD in children younger than 12 years of age is not different from that of adults, and that a similar response to intervention would be observed if a similar exposure was achieved, both adults and children are enrolled in the phase III study.

To predict drug exposure at different doses in children younger than 12 years of age, the PK structural model and the estimated fixed effects are considered to still be relevant, with only the demographic data derived using external

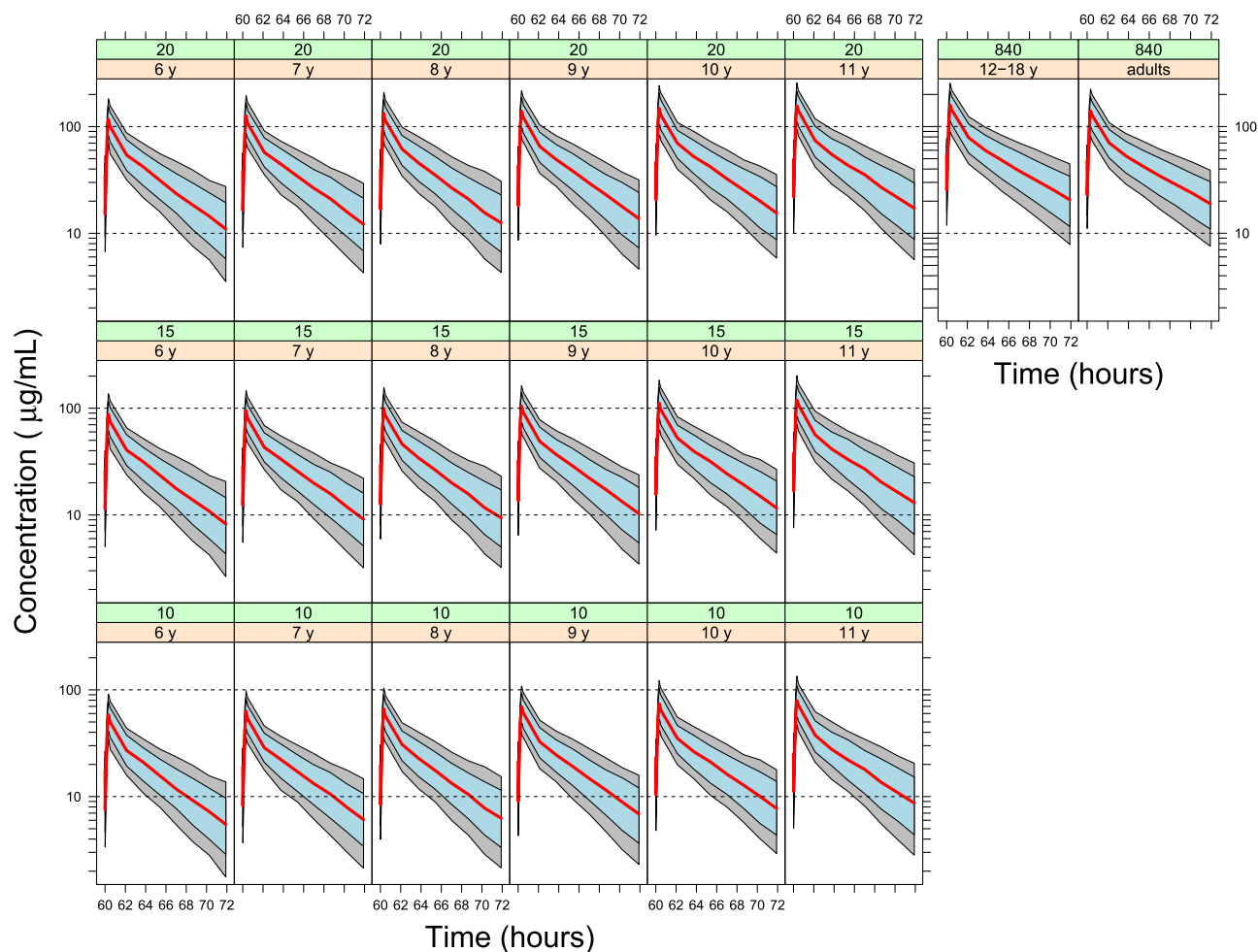


**Figure 5** Simulated concentration-time profiles after different dosing regimens in children aged 6–11 years with sickle cell disease compared with children aged 12–17 years and adults on a 1,680/840-mg fixed dosing regimen. Each row corresponds to one of the three dosing regimens in children and each column corresponds to a given year in age. Red lines indicate the median of the prediction interval, and the blue and gray areas correspond to 70% and 90% prediction intervals, respectively.

information. The CDC tables provided information to project height and weight growth curves. Differences between white subjects and black patients with SCD have been described in the article by Platt *et al.*,<sup>24</sup> allowing us to deviate from the CDC tables<sup>23</sup> as the primary source for demographic extrapolation to reflect a delay in growth. The patients with SCD may show further differences in clearance patterns, particularly as hyperfiltration has been widely discussed in SCD. As we had estimated a 23% greater clearance in patients in the phase II study, it is reasonable to assume that this factor may be attributed to hyperfiltration and would, therefore, also apply to younger children.

It was assumed that the scaling of CRCL was the main determinant for rivipansel clearance and, together with a body scale measure such as weight, will be sufficient to predict exposure.

The subsequent simulation exercise identified a dosing regimen of 40-mg/kg as a loading dose followed by 20-mg/kg every 12 hours as the maintenance dose for children aged 6–11 years. This should be sufficient to establish exposure ranges shown to be efficacious in the phase II study and to

exceed the prespecified target concentration of  $>10 \mu\text{g/mL}$ . The recommended dosing regimen of 40/20 mg/kg will also ensure that comparable concentration ranges are maintained across the age range, which will be important in interpreting future study results.

Because the relationship between CRCL and weight is not linear, weight-based dosing does not provide similar  $C_{\text{avg,ss}}$  across the whole age range for children 6–12 years old. In 6-year-old children, concentrations were predicted to be about 30% lower compared with adults; however, doses higher than 40 mg/kg could not be studied due to lack of preclinical toxicity information and, therefore, specifically in the younger children, higher doses were not applicable.

Finally, for the Jamaican SCD population that represents a typical target population, a growth delay would cause a slightly lower height compared with the height predictions from the CDC tables for the same age, resulting in a lower weight as well. That, in turn, given the weight-based dosing for children with SCD receiving rivipansel, would largely counteract potentially lower CRCL values.



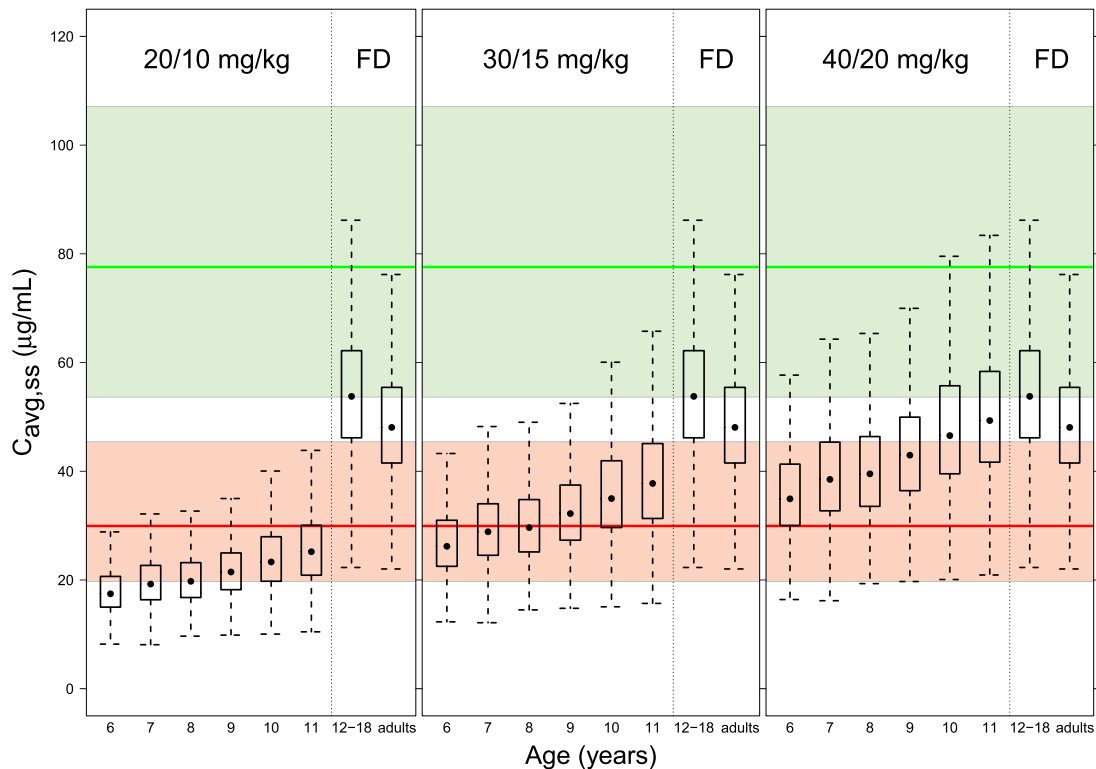


**Figure 6** The distribution of average concentrations within a dosing interval at steady-state ( $C_{avg,ss}$ ) with different dosing regimens across the age ranges to be studied in the phase III study. Each panel shows a dosing regimen in children compared to the fixed dosing (FD) regimen in adults of 1,680/840 mg. Left: 20/10-mg/kg; middle: 30/15-mg/kg; and right: 40/20-mg/kg. Distributions of  $C_{avg,ss}$  after the low dose (pink) and high dose (green), as observed in the phase II study,<sup>6</sup> are shown in the background, with the line indicating the median and the shaded area indicating the 95% prediction interval.

### Limitations

Some of the assumptions evolving from the modeling and simulation extrapolation exercise into this special population are discussed here. The use of the Schwartz formula for estimating GFR, like other serum creatinine-based formulas, is limited in SCD, as it tends to overestimate the GFR in these patients.<sup>10,33</sup> However, as it is commonly used by pediatricians, it was applied to this phase III model. One caveat in using the Schwartz formula is the fact that it was derived in children with CKD, where patients' GFR was estimated with a mean of 41 mL/min/1.73m<sup>2</sup>. In contrast, our SCD population will more likely resemble a largely normal GFR population, which may also be affected by hyperfiltration, with half of the children seeming to show some degree of hyperfiltration as indicated by their estimated glomerular filtration rate of >140 mL/min/1.73m<sup>2</sup>. The variable frequency of hyperfiltration across children with SCD was not accounted for in the simulations, which is largely beyond the scope for this publication and would need to be explored further. Although we assume all patients experience a similar degree of hyperfiltration, any lower frequency would result in a marginally lower clearance overall, which would unlikely be clinically relevant.

Because renal clearance is proportional to CRCL and not weight, an mg/kg dosing regimen would not lead to an exactly similar exposure across the age range of 6–11 years but was still chosen as the most feasible dosing regimen.

There is limited information available on the effective concentration threshold of 10 µg/mL as the target for minimum blood plasma concentration, as it is based on PK/pharmacodynamic modeling from preclinical studies. Finally, it is assumed that the pathophysiologic condition of the disease is similar across the whole age range. However, given that hyperfiltration is already being described in the younger population of patients with SCD, it is unknown how the development of the kidney function is influenced by the disease.

Although the simulations indicated that the 40/20-mg/kg dose would provide the best comparison to the phase II study data, it is important to note that the selection of pediatric dosing recommendations should be made while considering the PK results in the context of the safety and efficacy findings.

### CONCLUSIONS

A dosing recommendation comprising a 40-mg/kg loading dose followed by a maintenance dose of 20 mg/kg every 12 hours was selected for children aged 6–11 years participating in the ongoing phase III study (NCT02187003). This regimen was selected based on the evaluation of multiple dosing regimens likely required to achieve sufficient and similar exposure across the range of patient ages in the

study, and will provide acceptable concentration ranges shown to have been effective in phase II. This dosing regimen also accounts for the uncertainty in predictions for the lowest age range, for which the safety profile of rivipansel is not currently known. The ongoing phase III study will attempt to confirm the validity of the exposure predictions from this modeling and simulation exercise and also provide evidence of efficacy in the pediatric population at the proposed dosing regimen.

**Acknowledgments.** The authors thank Bina J. Patel, PharmD, and Teri O'Neill of Peloton Advantage, Parsippany, NJ, for editorial support, which was funded by Pfizer.

**Conflict of Interest.** B.K.T. and L.O.H. are employees of Pfizer.

**Source of Funding.** This study was sponsored by Pfizer. Editorial support was provided by Bina J. Patel, PharmD, and Teri O'Neill of Peloton Advantage, Parsippany, NJ, and was funded by Pfizer.

**Author Contributions.** B.K.T. and L.O.H. wrote the manuscript. B.K.T. and L.O.H. designed the research. B.K.T. and L.O.H. performed the research. B.K.T. and L.O.H. analyzed the data.

1. Schnog, J.B., Duits, A.J., Muskiet, F.A., ten Cate, H., Rojer, R.A. & Brandjes, D.P. Sickle cell disease; a general overview. *Neth. J. Med.* **62**, 364–374 (2004).
2. Frenette, P.S. & Atweh, G.F. Sickle cell disease: old discoveries, new concepts, and future promise. *J. Clin. Invest.* **117**, 850–858 (2007).
3. Kato, G.J., Hebbel, R.P., Steinberg, M.H. & Gladwin, M.T. Vasculopathy in sickle cell disease: biology, pathophysiology, genetics, translational medicine, and new research directions. *Am. J. Hematol.* **84**, 618–625 (2009).
4. Rees, D.C., Williams, T.N. & Gladwin, M.T. Sickle-cell disease. *Lancet* **376**, 2018–2031 (2010).
5. Okpala, I. Investigational selectin-targeted therapy of sickle cell disease. *Expert Opin. Investig. Drugs* **24**, 229–238 (2015).
6. Sparkenbaugh, E. & Pawlinski, R. Interplay between coagulation and vascular inflammation in sickle cell disease. *Br. J. Haematol.* **162**, 3–14 (2013).
7. Hebbel, R.P., Osarogiagbon, R. & Kaul, D. The endothelial biology of sickle cell disease: inflammation and a chronic vasculopathy. *Microcirculation* **11**, 129–151 (2004).
8. Turhan, A., Weiss, L.A., Mohandas, N., Coller, B.S. & Frenette, P.S. Primary role for adherent leukocytes in sickle cell vascular occlusion: a new paradigm. *Proc. Natl. Acad. Sci. USA* **99**, 3047–3051 (2002).
9. Kanter, J. & Kruse-Jarres, R. Management of sickle cell disease from childhood through adulthood. *Blood Rev.* **27**, 279–287 (2013).
10. Ware, R.E. *et al.* Renal function in infants with sickle cell anemia: baseline data from the BABY HUG trial. *J. Pediatr.* **156**, 66–70 (2010).
11. Aygun, B., Mortier, N.A., Smeltzer, M.P., Shulkin, B.L., Hankins, J.S. & Ware, R.E. Hydroxyurea treatment decreases glomerular hyperfiltration in children with sickle cell anemia. *Am. J. Hematol.* **88**, 116–119 (2013).
12. Audard, V., Bartolucci, P. & Stehlé, T. Sickle cell disease and albuminuria: recent advances in our understanding of sickle cell nephropathy. *Clin. Kidney J.* **10**, 475–478 (2017).
13. Telen, M.J. Beyond hydroxyurea: new and old drugs in the pipeline for sickle cell disease. *Blood* **127**, 810–819 (2016).

14. Tammara, B.K., Plotka, A., Shafer, F.E., Readett, D.R.J., Riley, S. & Korth-Bradley, J.M. Lack of effect of rivipansel on QTc interval in healthy adult African American male subjects. *J. Clin. Pharmacol.* **57**, 1315–1321 (2017).
15. Telen, M.J. *et al.* Randomized phase 2 study of GMI-1070 in SCD: reduction in time to resolution of vaso-occlusive events and decreased opioid use. *Blood* **125**, 2656–2664 (2015).
16. Wun, T. *et al.* Phase 1 study of the E-selectin inhibitor GMI 1070 in patients with sickle cell anemia. *PLoS One* **9**, e101301 (2014).
17. Dosne, A.G., Bergstrand, M., Harling, K. & Karlsson, M.O. Improving the estimation of parameter uncertainty distributions in nonlinear mixed effects models using sampling importance resampling. *J. Pharmacokinet. Pharmacodyn.* **43**, 583–596 (2016).
18. de Paula, R.P., Nascimento, A.F., Sousa, S.M., Bastos, P.R. & Barbosa, A.A. Glomerular filtration rate is altered in children with sickle cell disease: a comparison between Hb SS and Hb SC. *Rev. Bras. Hematol. Hemoter.* **35**, 349–351 (2013).
19. Hirschberg, R. Glomerular hyperfiltration in sickle cell disease. *Clin. J. Am. Soc. Nephrol.* **5**, 748–749 (2010).
20. Cockcroft, D.W. & Gault, M.H. Prediction of creatinine clearance from serum creatinine. *Nephron* **16**, 31–41 (1976).
21. Schwartz, G.J., Brion, L.P. & Spitzer, A. The use of plasma creatinine concentration for estimating glomerular filtration rate in infants, children, and adolescents. *Pediatr. Clin. North Am.* **34**, 571–590 (1987).
22. Dubois, D. & Dubois, E.F. Clinical calorimetry tenth paper. A formula to estimate the approximate surface area if height and weight be known. *JAMA Intern. Med.* **17**, 863–871 (1916).
23. Growth charts. Centers for Disease Control and Prevention 2009 10/21/2015. <[www.cdc.gov/growthcharts/percentile\\_data\\_files.htm](http://www.cdc.gov/growthcharts/percentile_data_files.htm)> (2009). Accessed 30 August 2016.
24. Platt, O.S., Rosenstock, W. & Espeland, M.A. Influence of sickle hemoglobinopathies on growth and development. *N. Engl. J. Med.* **311**, 7–12 (1984).
25. Thomas, P.W., Singhal, A., Hemmings-Kelly, M. & Serjeant, G.R. Height and weight reference curves for homozygous sickle cell disease. *Arch. Dis. Child.* **82**, 204–208 (2000).
26. Ceriotti, F. *et al.* Reference intervals for serum creatinine concentrations: assessment of available data for global application. *Clin. Chem.* **54**, 559–566 (2008).
27. Schlebusch, H., Liappis, N., Kalina, E. & Klein, C. High sensitive CRP and creatinine: reference intervals from infancy to childhood. *Lab. Med.* **26**, 341–346 (2002).
28. Hoste, L. *et al.* A new equation to estimate the glomerular filtration rate in children, adolescents and young adults. *Nephrol. Dial. Transplant.* **29**, 1082–1091 (2014).
29. Pediatric test reference values. Rochester, MN: Mayo Medical Laboratories, Mayo Clinic. 21 October 2015. <[www.mayomedicallaboratories.com/test-info/pediatric/ref-values/reference.php](http://www.mayomedicallaboratories.com/test-info/pediatric/ref-values/reference.php)> (2015). Accessed 30 August 2016.
30. Chang, J., Patton, J.T., Sarkar, A., Ernst, B., Magnani, J.L. & Frenette, P.S. GMI-1070, a novel pan-selectin antagonist, reverses acute vascular occlusions in sickle cell mice. *Blood* **116**, 1779–1786 (2010).
31. Pediatric science and research activities. US Food and Drug Administration. 21 October 2015. <[www.fda.gov/ScienceResearch/SpecialTopics/PediatricTherapeuticsResearch/ucm106614.htm](http://www.fda.gov/ScienceResearch/SpecialTopics/PediatricTherapeuticsResearch/ucm106614.htm)> (2015). Accessed 30 August 2016.
32. Selected normal pediatric laboratory values. 21 October 2015. <<http://wps.prenhall.com/wps/media/objects/354/362846/London%20App.%20B.pdf>> (2015). Accessed 30 August 2016.
33. Schwartz, G.J. *et al.* New equations to estimate GFR in children with CKD. *J. Am. Soc. Nephrol.* **20**, 629–637 (2009).

© 2017 The Authors CPT: Pharmacometrics & Systems Pharmacology published by Wiley Periodicals, Inc. on behalf of American Society for Clinical Pharmacology and Therapeutics. This is an open access article under the terms of the Creative Commons Attribution-NonCommercial-NoDerivs License, which permits use and distribution in any medium, provided the original work is properly cited, the use is non-commercial and no modifications or adaptations are made.

Supplementary information accompanies this paper on the CPT: Pharmacometrics & Systems Pharmacology website (<http://psp-journal.com>)